U.S. DEPARTMENT OF ENERGY

PNNL-25418

Prepared for the U.S. Department of Energy
under Contract DE-AC05-76RL01830

# Minimum Detectable Concentration and Concentration Calculations

Matthew W Cooper
James C Hayes
Brian T Schrom
James H Ely
Justin I McIntyre

May 2016

Pacific Northwest
NATIONAL LABORATORY

Proudly Operated by Battelle Since 1965

# Minimum Detectable Concentration and Concentration Calculations

Matthew W. Cooper
James H. Ely
James C. Hayes
Justin I. McIntyre
Brian T. Schrom

May 2016

Prepared for the U.S. Department of Energy

under Contract DE-AC06-76RL01830

## DISCLAIMER

This report was prepared as an account of work sponsored by an agency of the United States Government. Neither the United States Government nor any agency thereof, nor Battelle Memorial Institute, nor any of their employees, makes **any warranty, express or implied, or assumes any legal liability or responsibility for the accuracy, completeness, or usefulness of any information, apparatus, product, or process disclosed, or represents that its use would not infringe privately owned rights**. Reference herein to any specific commercial product, process, or service by trade name, trademark, manufacturer, or otherwise does not necessarily constitute or imply its endorsement, recommendation, or favoring by the United States Government or any agency thereof, or Battelle Memorial Institute. The views and opinions of authors expressed herein do not necessarily state or reflect those of the United States Government or any agency thereof.

PACIFIC NORTHWEST NATIONAL LABORATORY

*Operated by*

BATTELLE

*For the*

UNITED STATES DEPARTMENT OF ENERGY

*Under Contract DE-AC05-76RL01830*

# Contents



# Figures

# Executive Summary

This report highlights the work that has been completed on concentration calculations, uncertainties and minimum detectable concentration (MDC) for radioxenon collection systems. A discussion on the theory behind MDC calculations is given. In addition, regions of interest (ROI) and their role in correcting for both memory effects and interference terms are given in detail. A detailed derivation and walkthrough of the calculation is given with some discussion at each stage of the equation. Finally, some specific examples are given with typical numbers from an ARSA system as a guide.

IMS radionuclide stations, similar to the Automated Radioxenon Sampler/Analyzer (ARSA) developed at Pacific Northwest National Laboratory (PNNL), separate xenon gas from the sample collected. It uses a $\beta$-$\gamma$ coincidence detection system to determine xenon concentrations. This report describes the procedure used to determine the concentration, the concentration uncertainties and the minimum detectable concentration (MDC) levels for each of the radioxenon isotopes of interest. All of these calculations require knowledge of the ambient background, interference terms, background due to residual gas (memory effect), detection efficiencies, branching ratios, collection time, processing time, and acquisition time. In addition, there are terms and uncertainties that could be added to the calculations but have been omitted by choice. These omissions have been highlighted for the sake of completeness.

# Concentrations, Uncertainties and MDC

The concentrations of radioxenon are very important for the detection of nuclear explosions. In addition, the propagation of the uncertainties, both statistical and systematic, gives a measure of the confidence that one has in the concentrations measured. Finally, the MDC indicates what the combined collection and detection systems should be able to see in the absence of any actual radioxenon isotopes (i.e. the system fidelity). For some locations, such as islands in the southern hemisphere, the MDC may be the only reported measurement made on a daily basis during long periods of non-testing. As the MDC is the most difficult to understand and calculate we begin with a general description of the calculations given by Currie (1968). Essentially, there are three limits: critical level (LC), detection limit (LD) and determination limit (LQ). These three limits can be visualized in (1) (Currie 1968).

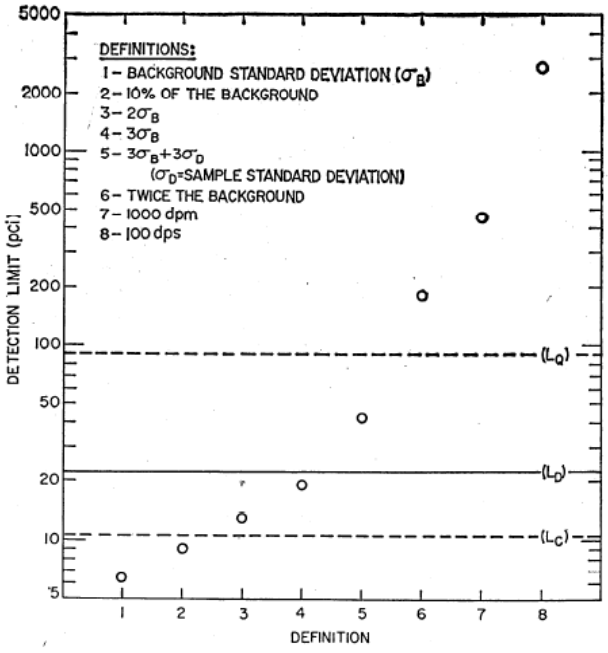


Figure 1: The detection limit for a specific radioactivity measurement process is plotted in increasing order. LC, LD, and LQ are the critical level, detection limit, and determination limit as described is Currie (1968).

$$L_C = k_\alpha \sigma_o \tag{1}$$

$$L_D = L_C + k_\beta \sigma_D \tag{2}$$

Where $k_\alpha$ and $k_\beta$ are the abscissa of the standardized normal distribution, with α (β) corresponding to the probability of false positive (negative) events. For this report $\alpha = \beta = 5\%$. Since $\sigma_D = \sqrt{L_D + \sigma_o^2}$, the detection limit can be rewritten as

$$L_D = L_C + k_\beta \sqrt{L_D + \sigma_o^2} \tag{3}$$

After expanding and solving for $L_D$ one gets

$$L_D = L_C + k_\beta\left(1+\sqrt{1+\frac{4L_C}{k_\beta^2}+\frac{4L_C^2}{k_\beta^2 k_\alpha^2}}\right) \tag{4}$$

Since $k_\alpha = k_\beta$, (4) is simplified to

$$L_D = 2L_C + k^2 \tag{5}$$

After substituting (1) into (5)

$$L_D = k^2 + 2k\sigma_o \tag{6}$$

In the case where $k = 1.645$

$$L_D = 2.71 + 4.65\sigma_o \tag{7}$$

Where,

$$\sigma_o = \sqrt{BckCnt + \sigma^2_{BckCnt} + InterferenceCnt + \sigma^2_{InterferenceCnt} + MemoryCnt + \sigma^2_{MemoryCnt}} \tag{8}$$

The six terms are determined from three data sets: detector background, gas background, and sample. The count terms (*Cnt*) are purely statistical in nature and a derived from simple photo-statics while the $\sigma^2$ terms arise from both statistical and systematic effects. All the terms are simplified and are shown to indicate what components are present. This allows one to write the general form for MDC,

$$MDC\left(\frac{mBq}{m^3 air}\right) = \left(\frac{2.71+4.65\sigma_0}{\varepsilon_\gamma \varepsilon_\beta \gamma_{BR} \beta_{BR}}\right)\frac{\lambda^2 * T_C}{(1-\exp(-\lambda T_C))\exp(-\lambda T_P)(1-\exp(-\lambda T_A))}\left(\frac{1000}{V_{Air}}\right) \tag{9}$$

where,

$$\begin{aligned}
\sigma_0 &= \sqrt{BckCnt + \sigma^2_{BckCnt} + InterferenceCnt + \sigma^2_{InterferenceCnt} + MemoryCnt + \sigma^2_{MemoryCnt}} = L_C \\
\varepsilon_\gamma &= \gamma\ Efficiency \\
\varepsilon_\beta &= \beta\ Efficiency \\
\gamma_{BR} &= \gamma\ Branching\ Ratio \\
\beta_{BR} &= \beta\ Branching\ Ratio \\
\lambda &= Ln(2)/t_{\frac{1}{2}} \\
T_C &= Xenon\ Collection\ Time \\
T_P &= Processing\ Time\ of\ Gas \\
T_A &= Acquisition\ Time\ of\ Counts \\
V_{Air} &= cc\ of\ Xenon/0.087\ cc\ of\ Xenon\ per\ m^3 air
\end{aligned}$$

The first term (red) in (9) contains the nuclear physics that pertains directly to the detector. The second term (orange) takes into account the radioactive decay of the particular nucleus. Contained in the second term is $\frac{\lambda * T_C}{1-\exp(-\lambda T_C)}$, which is a saturation term. It represents the collection of the radioactive sample

from the atmosphere. The collection is assumed to be constant activity collected in a linear fashion. In systems that use a pre-collected sample the second term goes to 1. $T_C$ is the collection of the radioxenon in the sphere, while $T_P$ is the time from collection stop to detector acquisition start. The $T_A$ term is the acquisition time of the sample. The last term (yellow) converts the rate into the proper units, $\frac{mBq}{m^3}$.

## Regions of Interest (ROI)

The three data sets can be further broken down into what the data is comprised. The sample file contains the data from the sample plus memory plus ambient background. The gas background contains the memory effect from the previous runs and the ambient background. Finally, the detector background should contain only the ambient background.

The seven regions of interest (ROI) are defined by a range in both γ and β energy. The regions are $^{214}$Pb (ROI-1), $^{135}$Xe (ROI-2), $^{133}$Xe (ROI-3), $^{133}$Xe (ROI-4), $^{131m}$Xe (ROI-5), $^{133m}$Xe (ROI-6), and an exclusion (ROI-7) region (Figure 2). Each region spans in both γ energy range and β energy range. Each region corresponds to an important β-γ signature or combinations of signatures for each isotope. The $^{214}$Pb region (ROI-1) contains just radon daughter products and no radioxenon isotopes. The $^{135}$Xe (ROI-2) and $^{133}$Xe (ROI-3) regions are free from interferences of the other radioxenon isotopes. There is some small contribution (~2%) from Compton scatter from $^{135}$Xe into ROI-3, but this contribution has been ignored for the sake of these calculations. Regions 4, 5, 6, and 7 are admixtures of $^{133}$Xe, $^{131m}$Xe and $^{133m}$Xe. ROI-7 represents a region with maximal possibility of meta-stable ($^{131m}$Xe and $^{133m}$Xe) interference while ROI-4 minus ROI-7 represents a pure $^{133}$Xe signature.

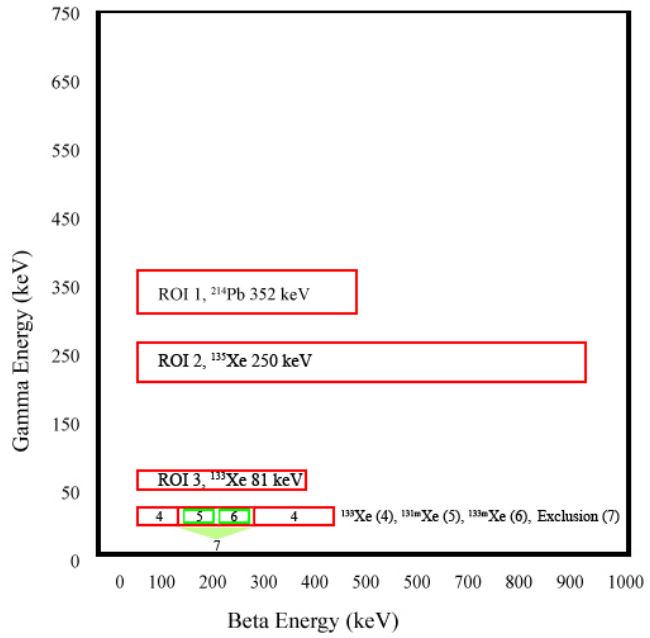


Figure 2: Placement of the 7 regions of interest (ROI).

Ratios of the ROIs account for interference from Radon daughters (Figure 3) as well as the two metastables. There are ratios taken between ROI-1 and the six other ROI (1:2, 1:3, 1:4, 1:5 1:6, and 1:7). The radon daughter ratios are important since they cause interference with $^{135}$Xe, $^{133}$Xe, $^{133m}$Xe, and $^{131m}$Xe. The counts due to the interference are subtracted out. Using a pure spike of radon (daughter products $^{214}$Pb and $^{214}$Bi) allows the determination of the interference ratios for each of the ROI's. For the radon, the ratios are taken between ROI-1 and the six other ROI (1:2, 1:3, 1:4, 1:5 1:6, and 1:7). The other important interference ratios are based on $^{133}$Xe (Figure 4) in the ROI's of the two metastables. Here the ratios are 3:4, 3:5, 3:6, 3:7, and 3:(4-7). The 3:4 ratio is important for the case where there are no metastables. The 3:5 and 3:6 ratios are important when there are metastables present. Finally, the 3:7 and 3:(4-7) are important for determining if there are metastables present at all. The last interference term is $^{135}$Xe, which uses the ratios of ROI-2 to all lower ROI's. The $^{135}$Xe ratios account for Compton scatter and the ~30 keV x-ray/β coincidence that interferes with ROI-4 and -6. For all of the following calculations it is critical to subtract out the interference terms using the appropriate ratio.

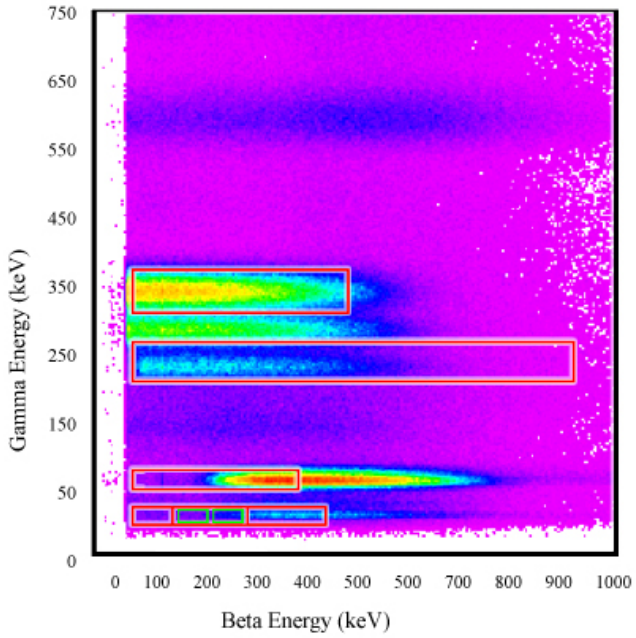


Figure 3: A radon spike used to determine interference ratios with the ROI's overlaid.

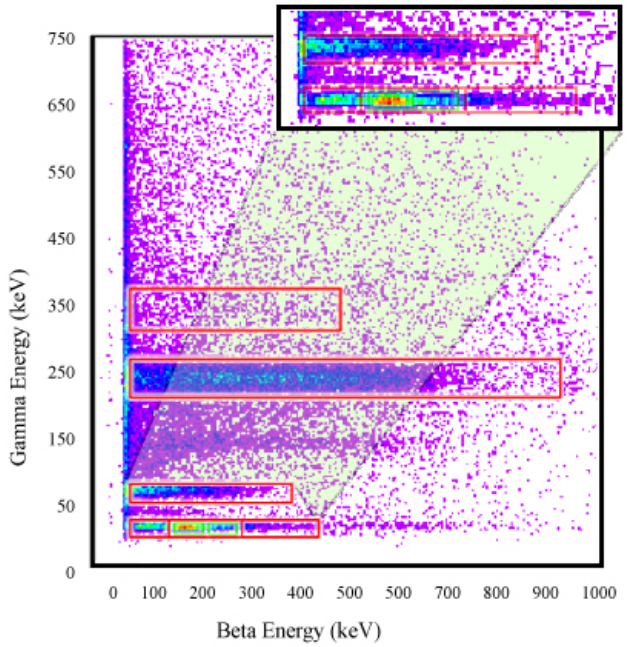


Figure 4: $^{135}$Xe spike used for determination of $^{133}$Xe ROI ratios with ROI's overlaid. The upper right figure is an expanded view of the lower left section.

# LC Calculation

The first step taken in the analysis is to correct for dead time. The dead-time is corrected by taking a ratio of the real-time (RT) to live-time (LT).

$$D_{Raw:ROIn} = Bkgd_{Raw:ROIn} * \frac{RT_D}{LT_D} \tag{10}$$

$$\sigma_{D_{Raw:ROIn}} = \frac{RT_D}{LT_D} * \sqrt{Bkgd_{Raw:ROIn}} \tag{11}$$

$$G_{Raw:ROIn} = Gas_{Raw:ROIn} * \frac{RT_G}{LT_G} \tag{12}$$

$$\sigma_{G_{Raw:ROIn}} = \frac{RT_G}{LT_G} * \sqrt{Gas_{Raw:ROIn}} \tag{13}$$

$$S_{Raw:ROIn} = Sam_{Raw:ROIn} * \frac{RT_S}{LT_S} \tag{14}$$

$$\sigma_{S_{Raw:ROIn}} = \frac{RT_S}{LT_S} * \sqrt{Sam_{Raw:ROIn}} \tag{15}$$

Subtract the detector background from both the sample and gas background. The sample is composed of ambient background, memory effects from previous samples, and the actual sample of interest. The gas background data (Figure 5) is composed of ambient background and the memory effect from previous samples. The detector background data is composed of only the ambient background (Figure 6). The detector background is measured during the first three days of operation of the system at a new site.

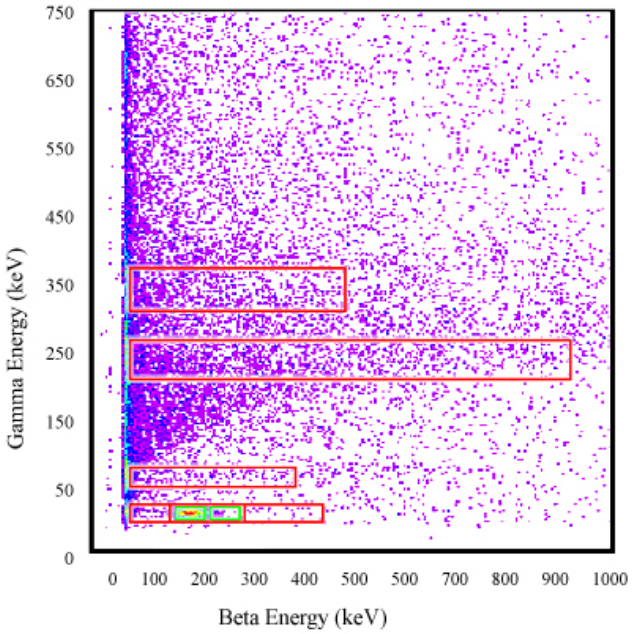


Figure 5: A gas background after a medical isotope ($^{133}$Xe, $^{131m}$Xe) spike with ROI's overlaid.

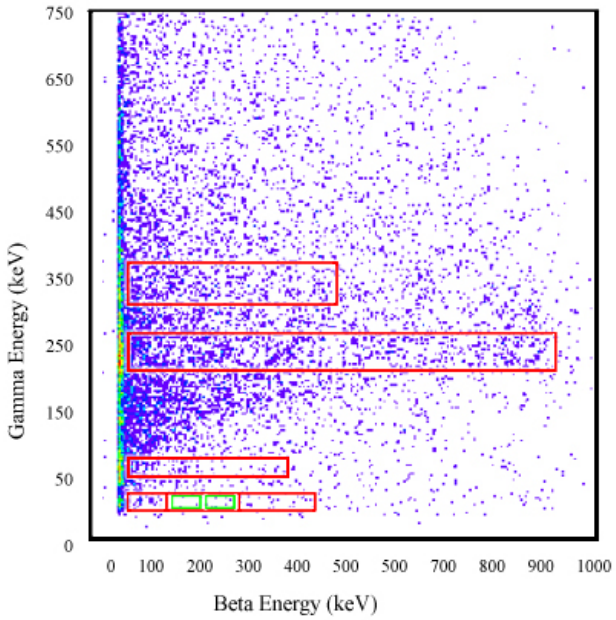


Figure 6: An example of a detector background data set with ROI's overlaid.

By subtracting, the detector background from the gas background (sample) the data set is reduced to only containing the memory effect (memory and sample). Each file used in the calculation accounts for different periods; for example, the Automated Radioxenon Sampler/ Analyzer (ARSA) uses 72-hrs for a detector background, 8-hours for a typical gas background and 24-hours for a typical sample. The detector background will be normalized to real-time acquisition interval ($\Delta T_S$, $\Delta T_G$, and $\Delta T_D$) from which it will be subtracted.

$$D_{SROIn} = D_{Raw:ROIn} * \frac{\Delta T_S}{\Delta T_D} \tag{16}$$

$$\sigma_{D_{SROIn}} = \frac{\Delta T_S}{\Delta T_D} * \sqrt{D_{Raw:ROIn}} \tag{17}$$

$$D_{GROIn} = D_{Raw:ROIn} * \frac{\Delta T_G}{\Delta T_D} \tag{18}$$

$$\sigma_{D_{GROIn}} = \frac{\Delta T_G}{\Delta T_D} * \sqrt{D_{Raw:ROIn}} \tag{19}$$

An example of the three times: $\Delta T_S$, $\Delta T_G$ and $\Delta T_D$ along with decay of the four primary radioxenon isotopes is depicted in Figure 7. Once the data sets have been time adjusted to same time interval as the sample, the ROI time corrected detector counts, (16), is subtracted from the respective ROI in both the time corrected gas background and sample data sets as seen in (20) and (22).

$$S_{ROIn} = S_{RawROIn} - D_{SROIn} \tag{20}$$

$$\sigma_{S_{ROIn}} = \sqrt{\sigma^2_{S_{Raw:ROIn}} + \sigma^2_{D_{SROIn}}} \tag{21}$$

$$G_{ROIn} = G_{Raw:ROIn} - D_{GROIn} \tag{22}$$

$$\sigma_{G_{ROIn}} = \sqrt{\sigma^2_{G_{Raw:ROIn}} + \sigma^2_{D_{GROIn}}} \tag{23}$$

The use of a long detector-background count time is important to minimize the uncertainties associated with this measurement, i.e. longer counts times give smaller relative uncertainties.

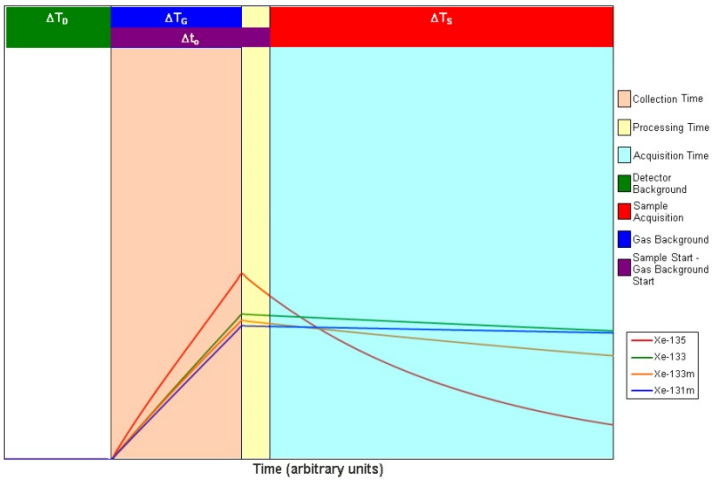


Figure 7: Shows the chemistry timeline (vertical colored bands), detector acquisition (top timeline), and an example of the isotope activity (given by the four lines in the bottom of the figure) present in a typical radioxenon system. In currently developed systems the measurement is corrected to a $T_o$ of collection stop. The detector background (the section marked with a green horizontal bar) is the first data collected, which on this scale is too small to be displayed. The four regions: white, orange, yellow, and light blue show the number of decays at a given time. The white region (background) contains only decays from the ambient background and gas background (memory effect). The orange region (collection) assumes a linear increase in the number on radioxenon present, so there are an increasing number of decays as one goes forward in time. The yellow region (processing) represents the time between collection and data acquisition, so there is no added radioxenon and only decay. In the last region, light blue (acquisition), there is only decay of the radioxenon present. The top timeline shows what stage of acquisition the detector is in during any given chemistry stage of the system.

Another source of uncertainty in the measurement is from interference from one isotope to another. This can be in the form of radon or xenon. Radon interference must be subtracted from both the sample and gas background. This is done, in the case of radon, by using the ratio counts from ROI-1 and then subtract from the corresponding ROI. For the cases where $^{133}$Xe is an interference term, the ratio counts from ROI-3 are subtracted from the corresponding ROI. It is worth noting that in cases where there is either no radon or no xenon interference these terms will be zero within statistical uncertainties (i.e. Ratio = 0 and $\sigma_{ratio} = 0$). Of further importance is the need to subtract the gas background, detector background, and interference terms from ROI-3 before using the ratio of ROI-3 as an interference term for other regions.

$$Interference_{S_{Rn}} = S_{ROI1} * Ratio_{1:n} \tag{24}$$

$$\sigma_{Interference_{S_{Rn}}} = \sqrt{S_{ROI1}^2 * \sigma_{Ratio_{1:n}}^2 + \sigma_{S_{ROI1}}^2 * Ratio_{1:n}^2} \tag{25}$$

$$Interference_{S_{Xe135}} = \left(S_{ROI2} - S_{ROI1} * Ratio_{1:2}\right) * Ratio_{2:n} \tag{26}$$

$$\sigma_{Interference_{S_{Xe135}}} = \sqrt{\left(S_{ROI2} - S_{ROI1} \cdot Ratio_{1:2}\right)^2 \cdot \sigma_{Ratio_{2:n}}^2 + \left(\sigma_{S_{ROI2}}^2 + \sigma_{Interference_{S_{Rn}}}^2\right) \cdot Ratio_{2:n}^2} \tag{27}$$

$$Interference_{S_{Xe133}} = \left(S_{ROI3} - Interference_{S_{Xe135}} - Interference_{S_{Rn}}\right) * Ratio_{3:n} \tag{28}$$

$$\sigma_{Interference_{S_{Xe133}}} = \sqrt{\left(S_{ROI3} - Interference_{S_{Xe135}} - Interference_{S_{Rn}}\right)^2 \cdot \sigma_{Ratio_{3:n}}^2 + \left(\sigma_{S_{ROI3}}^2 + \sigma_{Interference_{S_{Xe135}}}^2 + \sigma_{Interference_{S_{Rn}}}^2\right) \cdot Ratio_{3:n}^2} \tag{29}$$

$$S_{Corrected_{ROIn}} = S_{ROIn} - Interference_{S_{Xe133}} - Interference_{S_{Xe135}} - Interference_{S_{Rn}} \quad (30)$$

$$\sigma_{S_{Corrected_{ROIn}}} = \sqrt{\sigma^2_{S_{ROIn}} + \sigma^2_{Interference_{S_{Rn}}} + \sigma^2_{Interference_{S_{Xe135}}} + \sigma^2_{Interference_{S_{Xe133}}}} \quad (31)$$

$$Interference_{S_{Rn}} = G_{ROI1} * Ratio_{1:n} \quad (32)$$

$$\sigma_{Interference_{G_{Rn}}} = \sqrt{G^2_{ROI1} * \sigma^2_{Ratio_{1:n}} + \sigma^2_{G_{ROI1}} * Ratio^2_{1:n}} \quad (33)$$

$$Interference_{G_{Xe135}} = \left(G_{ROI2} - G_{ROI1} * Ratio_{1:2}\right) * Ratio_{2:n} \quad (34)$$

$$\sigma_{Interference_{G_{Xe135}}} = \sqrt{\left(G_{ROI2} - G_{ROI1} \cdot Ratio_{1:2}\right)^2 \cdot \sigma^2_{Ratio_{2:n}} + \left(\sigma^2_{G_{ROI2}} + \sigma^2_{Interference_{G_{Rn}}}\right) \cdot Ratio^2_{2:n}} \quad (35)$$

$$Interference_{G_{Xe133}} = \left(G_{ROI3} - Interference_{G_{Xe135}} - Interference_{G_{Rn}}\right) * Ratio_{3:n} \quad (36)$$

$$\sigma_{Interference_{G_{Xe133}}} = \sqrt{\left(S_{ROI3} - Interference_{G_{Xe135}} - Interference_{G_{Rn}}\right)^2 \cdot \sigma^2_{Ratio_{3:n}} + \left(\sigma^2_{G_{ROI3}} + \sigma^2_{Interference_{G_{Xe135}}} + \sigma^2_{Interference_{G_{Rn}}}\right) \cdot Ratio^2_{3:n}} \quad (37)$$

$$G_{Corrected_{ROIn}} = G_{ROIn} - Interference_{G_{Xe133}} - Interference_{G_{Xe135}} - Interference_{G_{Rn}} \quad (38)$$

$$\sigma_{G_{Corrected_{ROIn}}} = \sqrt{\sigma^2_{G_{ROIn}} + \sigma^2_{Interference_{G_{Rn}}} + \sigma^2_{Interference_{G_{Xe135}}} + \sigma^2_{Interference_{G_{Xe133}}}} \quad (39)$$

Note that both the number of counts in ROI-1 and the uncertainty of the appropriate ratio (Ratio1:n) contribute to the uncertainty in the interference term. While the statistical uncertainty related to the number of counts in the gas background and the sample is determined from the square root of the counts and hence is variable and can be large in both relative terms and absolute terms, the uncertainty associated with the ratio can be made to be small during calibration. By using a high activity sample, several 10's to 100's of counts per second, it is possible to have the ratio uncertainty less than 0.5%.

An additional note is the inclusion of a switch that allows the operator to turn on or off the use of the radon ratio's and hence radon subtraction. While it was felt at discussions during the Stockholm Noble Gas workshop of 2005 that there should be no option to turn the radon subtraction on and off via $L_c$ calculations or through the use of an operator controlled switch, there are systems that have shown no radon interferences. Because such a system would be penalized in both the uncertainties and the MDC values for the inclusion of the radon ratio it has been determined that an operator controlled switch should be allowed, but no internal switch determined by an $L_c$ calculation should be allowed. It is also important to note that, with careful determination of the radon ratios, the inclusion of radon should have less than a 2% absolute effect on the concentrations, uncertainties, and MDC values.

Continuing with the determination of the concentration and associated uncertainty, subtract the gas background from the sample. Since the gas background is a measure of any residual isotopes present

from previous samples, the gas background (Eq. 34) needs to be half-life corrected (See Figure 7 for example decay curves) for each ROI.

$$Memory_{G:ROIn} = \frac{G_{Corrected_{ROIn}} * e^{-\lambda_n \Delta t_o}}{1 - e^{-\lambda_n * \Delta T_G}} \left(1 - e^{-\lambda_n * \Delta T_S}\right) \tag{40}$$

$$\sigma_{Memory_{G:ROIn}} = \frac{\sigma_{G_{Corrected_{ROIn}}} * e^{-\lambda_n \Delta t_o}}{1 - e^{-\lambda_n * \Delta T_G}} \left(1 - e^{-\lambda_n * \Delta T_S}\right) \tag{41}$$

Where,

$$\Delta t_o = (\text{Sample acquisition start time}) - (\text{Gas acquisition start time})$$

$$\Delta T_G = \text{Gas background acquisition time}$$

$$\Delta T_S = \text{Sample acquisition time}$$

$$\lambda_n = \text{Isotope decay constant}$$

At this point, it is possible to calculate $L_C$ for both the detector background, interference term, and gas background. Detector $L_C$ is simply

$$\sigma_{o_{Det}} = \sqrt{D_{ROIn} + \sigma^2_{D_{ROIn}}} \tag{42}$$

$$\sigma_{o_{Interference}} = \sqrt{Interference_{Rn:S} + \sigma^2_{Interference_{Rn:S}} + Interference_{Xe:S} + \sigma^2_{Interference_{Xe:s}}} \tag{43}$$

while, $L_{C_G}$ is

$$\sigma_{o_G} = \sqrt{Memory_{G:ROIn} + \sigma^2_{Memory_{G:ROIn}}} \tag{44}$$

For the definition of $\sigma_{o,}$ see equations (7) and (8).

$$\sigma_o^2 = \sigma^2_{o_D} + \sigma^2_{o_G} + \sigma^2_{o_{Interference}} \tag{45}$$

The MDC is calculated for each ROI using (44) and the base (9).

$$MDC\left(\frac{mBq}{m^3 air}\right) = \left(\frac{2.71 + 4.65\sigma_o}{\varepsilon_\gamma \varepsilon_\beta BR_\gamma BR_\beta}\right) \frac{\lambda^2 * T_C}{(1 - \exp(-\lambda T_C))\exp(-\lambda T_P)(1 - \exp(-\lambda T_A))} \left(\frac{1000}{V_{Air}}\right) \tag{46}$$

At this point, subtract the gas-background half-life corrected counts from the corresponding sample ROI counts (see (30) and (40)).

$$S_{f_{ROIn}} = S_{Corrected_{ROIn}} - Memory_{G:ROIn} \quad (47)$$

$$\sigma_{S_{f_{ROIn}}} = \sqrt{\sigma^2_{S_{Corrected_{ROIn}}} + \sigma^2_{Memory_{G:ROIn}}} \quad (48)$$

The concentration is calculated for each given ROI using equation (49).

$$Concentration\left(\frac{mBq}{m^3 air}\right) = \frac{S_{f_{ROIn}}}{\varepsilon_\gamma \varepsilon_\beta \gamma_{BR} \beta_{BR}} \frac{\lambda^2}{\left(1-\exp(-\lambda T_C)\right)\exp(-\lambda T_P)\left(1-\exp(-\lambda T_A)\right)} \frac{T_C * 1000}{V_{Air}}, \quad (49)$$

$$Error\left(\frac{mBq}{m^3 air}\right) = Concentration * \sqrt{\left(\frac{\sigma_{S_{f_{ROIn}}}}{S_{f_{ROIn}}}\right)^2 + \left(\frac{\sigma_{\varepsilon_\gamma}}{\varepsilon_\gamma}\right)^2 + \left(\frac{\sigma_{\varepsilon_\beta}}{\varepsilon_\beta}\right)^2 + \left(\frac{\sigma_{\beta_{BR}}}{\beta_{BR}}\right)^2 + \left(\frac{\sigma_{\gamma_{BR}}}{\gamma_{BR}}\right)^2 + \left(\frac{\sigma_{V_{Air}}}{V_{Air}}\right)^2} \quad (50)$$

# Specific Cases

## $^{135}$Xe

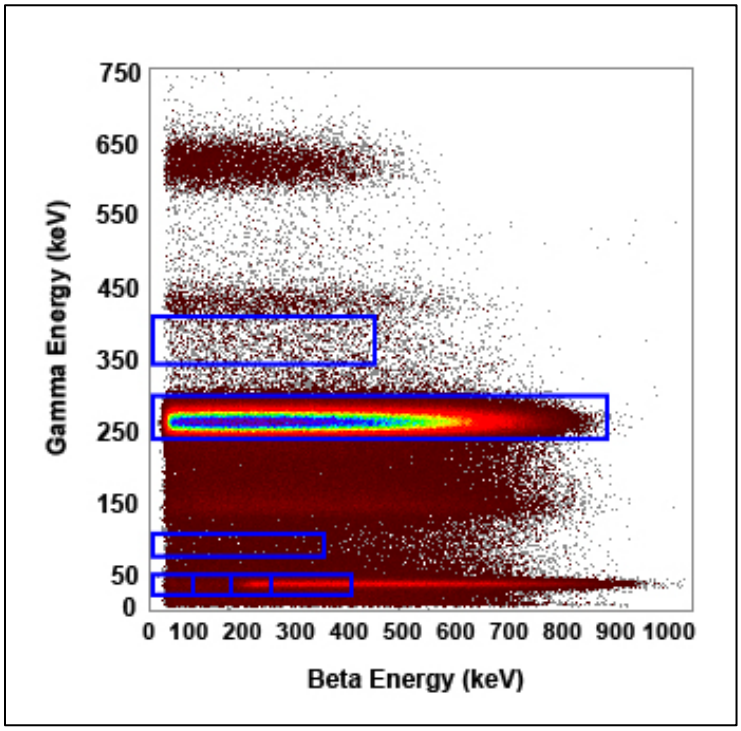


Figure 8: A sample file in which $^{135}$Xe is present.

$$^{135}Xe^{250}_{MDC}\left(\frac{mBq}{m^3 air}\right) = \frac{2.71 + 3.29\sigma^{135Xe}}{\varepsilon_\gamma \varepsilon_\beta \gamma_{BR} \beta_{BR}} \frac{\left(\lambda^{135Xe}\right)^2}{\left(1-\exp\left(-\lambda^{135Xe} T_C\right)\right)\exp\left(-\lambda^{135Xe} T_P\right)\left(1-\exp\left(-\lambda^{135Xe} T_A\right)\right)} \frac{T_C * 1000}{V_{Air}} \quad (51)$$

$\sigma^{135Xe}$ is calculated using Eq. 8 where the only interference occurs with radon.

$$\sigma^{135Xe} = \sqrt{2*\left(\sigma^{135Xe}_{BckCnt}\right)^2 + \left(Ratio^{135Xe}_{214Pb} * \sigma^{214Pb}_{SamCnt}\right)^2 + \left(\sigma_{Ratio^{135Xe}_{214Pb}} * SamCnts^{214Pb}\right)^2} \quad (52)$$

Where,

$$\sigma^{135Xe}_{BckCnt} = \sqrt{Counts_{Gas(Sam):ROI\,2}} \quad (53)$$

In this case, it is assumed that the uncertainties in timing and half-life are negligible. In addition, the half-life correction of the previous $^{135}$Xe is ignored since it has less than a 0.8% contribution.

$$\sigma^{214Pb}_{SamCnt} = \sqrt{BckCnts^{214Pb352} + SamCnts^{214Pb352}} \quad (54)$$

Furthermore, the interference term should only include radon interferences, so eq. 39 simplifies.

## $^{133}$Xe

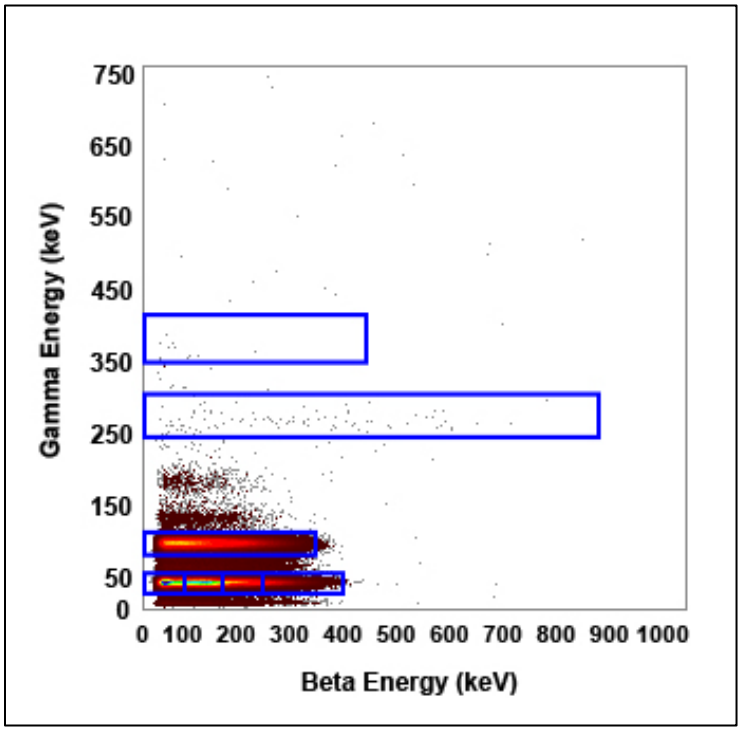


Figure 9: A sample file in which 133Xe is present.

For $^{133}$Xe, there are two ROI, 3 and 4. ROI-3 has the events with the 81-keV γ-ray in coincidence, while ROI-4 has the 30-keV x-ray in coincidence. ROI-4 also has two potential interference terms from the $^{131m}$Xe and $^{133m}$Xe. The MDC for the 81-keV ROI is calculated the same as $^{135}$Xe, discussed in the previous section.

$$^{133}Xe^{81}_{MDC}\left(\frac{mBq}{m^3 air}\right)=\frac{2.71+3.29\sigma^{133Xe81}}{\varepsilon_\gamma \varepsilon_\beta \gamma_{BR} \beta_{BR}} \frac{\left(\lambda^{133Xe}\right)^2}{\left(1-\exp\left(-\lambda^{133Xe}T_C\right)\right)\exp\left(-\lambda^{133Xe}T_P\right)\left(1-\exp\left(-\lambda^{133Xe}T_A\right)\right)} \frac{T_C * 1000}{V_{Air}} \quad (55)$$

Where,

$$\sigma^{133Xe81}=\sqrt{2*\left(\sigma^{133Xe81}_{BckCnt}\right)^2+\left(Ratio^{133Xe81}_{214Pb79}*\sigma^{214Pb79}_{SamCnt}\right)^2+\left(\sigma_{Ratio^{133Xe81}_{214Pb79}}*SamCnts^{214Pb79}\right)^2} \quad (56)$$

,

and

$$\sigma^{133Xe81}_{BckCnt}=\sqrt{BckCnts^{133Xe81}} \quad (57)$$

$$\sigma^{214Pb79}_{SamCnt}=\sqrt{BckCnts^{214Pb325}+SamCnts^{214Pb352}} \quad (58)$$

However, the MDC for the 30-keV ROI is calculated two ways. The first is the same as the 81-keV ROI, because the metastable states are assumed to be missing (uses the entire ROI-4). The second method uses only the sections of ROI-4 that do not overlap with the exclusion region (ROI-7).

$$\sigma^{133Xe30}=\sqrt{2*\left(\sigma^{133Xe30}_{BckCnt}\right)^2} \quad (59)$$

Where,

$$\sigma^{133Xe30}_{BckCnt}=\sqrt{BckCnts^{133Xe30}} \quad (60)$$

and the MDC is:

$$^{133}Xe^{30}_{MDC}\left(\frac{mBq}{m^3 air}\right)=\frac{2.71+3.29\sigma^{133Xe30}}{\varepsilon_\gamma \varepsilon_\beta \gamma_{BR} \beta_{BR}} \frac{\left(\lambda^{133Xe}\right)^2}{\left(1-\exp\left(-\lambda^{133Xe}T_C\right)\right)\exp\left(-\lambda^{133Xe}T_P\right)\left(1-\exp\left(-\lambda^{133Xe}T_A\right)\right)} \frac{T_C * 1000}{V_{Air}} \quad (61)$$

The two MDC calculations made for $^{133}$Xe can be combined to produce a single MDC for each spectrum. The equation,

$$^{133}Xe_{MDC}\left(\frac{mBq}{m^3 air}\right)=\sqrt{\frac{1}{\left(^{133}Xe^{81keV}_{MDC}\right)^{-2}+\left(^{133}Xe^{30keV}_{MDC}\right)^{-2}}} \quad (62)$$

is the weighted average of the uncertainties and is dominated by the smaller of the two MDC calculations. It should be noted that the equation used above is not mathematically rigorous, but within 10% of the rigorous value.

## $^{131m}$Xe

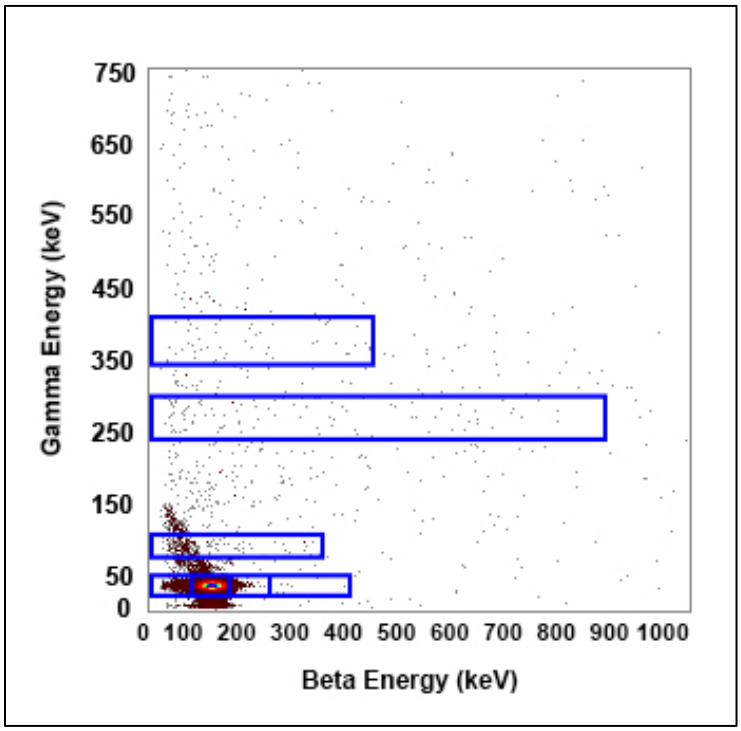


Figure 10: A sample file in which 131mXe is present.

For $^{131m}$Xe, the interference terms are due to $^{133}$Xe.

$$SamCnts^{131mXe30} = Cnt_{\mathrm{ROI}_5} - Cnt_{\mathrm{ROI}_3} * Ratio_{3:5} \tag{63}$$

$$\sigma^{131mXe30} = \sqrt{2*\left(\sigma_{BckCnt}^{\mathrm{ROI5}}\right)^2 + \left(Ratio_{3:5} * \sigma_{Cnt_{ROI3}}\right)^2 + \left(\sigma_{Ratio_{3:5}} * Cnt_{ROI3}\right)^2} \tag{64}$$

Where,

$$\sigma_{BckCnt}^{\mathrm{ROI5}} = \sqrt{BckCnts_{\mathrm{ROI5}}} \text{ and } \sigma_{Cnt_{ROI4}} = \sqrt{SamCnts^{\mathrm{ROI3}} + BckCnts^{\mathrm{ROI3}}} \tag{65}$$

The MDC is then:

$$^{131m}Xe_{MDC}^{30}\left(\frac{mBq}{m^3 air}\right) = \frac{2.71 + 3.29\sigma^{131mXe30}}{\varepsilon_\gamma \varepsilon_\beta \gamma_{BR} \beta_{BR}} \frac{\left(\lambda^{131mXe}\right)^2}{\left(1-\exp\left(-\lambda^{131mXe}T_C\right)\right)\exp\left(-\lambda^{131mXe}T_P\right)\left(1-\exp\left(-\lambda^{131mXe}T_A\right)\right)} \frac{T_C * 1000}{V_{Air}} \tag{66}$$

Similarly, $^{133m}$Xe is done in the same fashion. In this case ROI-6 is used instead of ROI-5.

# Conclusion

Concentration with uncertainty and MDC calculations can be very complex, however with some assumptions they can be simplified considerably without significant impact on the uncertainty of the calculation. In the case beta-gamma radioxenon systems it is very important to account for ambient background, memory effect, and interference. These different components are obtained by different combinations of the three data files: detector background, gas background, and sample. In the end, to obtain the most accurate results it is very important to have a well characterized detector.